Neurology Asia 2026; 31(2) : 709 – 722

Virtual reality technology for the treatment of mild cognitive impairment: Changes in immune-related genes and alternative splicing and implications for treatment efficacy

[1]Nazuke Yusupu, [2]Hongyan Li

[1]Xinjiang Medical University, Urumqi, China; [2]Neurology diagnosis and treatment center, People's Hospital of Xinjiang Uygur Autonomous Region; Xinjiang Clinical Research Center for Stroke and Neurological Rare Disease, Xinjiang National center for cognitive disorders, Urumqi, China

Abstract

Background: Mild Cognitive Impairment (MCI) is recognized as a critical transitional stage from the preclinical phase of Alzheimer's Disease (AD) to overt dementia, while AD is a progressive neurodegenerative disorder with limited therapeutic options. Virtual Reality (VR) therapy has emerged as a promising non-pharmacological intervention for cognitive disorders. The purpose of this study was to investigate the molecular mechanisms underlying VR therapy in AD-MCI. *Methods:* RNA sequencing was performed on peripheral blood mononuclear cells (PBMCs) from healthy volunteers (C, n=5), AD-MCI patients before VR intervention (ADB, n=5), and after completion of the VR-based Cognitive Rehabilitation Software (VR-CRS) program (ADA, n=3). We conducted differential expression analysis, functional enrichment and trend clustering of genes. Alternative splicing events were also analyzed and co-expression networks were constructed with RNA-binding proteins. *Results:* Principal component analysis revealed a distinct shift in the global gene expression profile following VR-CRS intervention. Differential expression analysis identified 421 upregulated and 186 downregulated genes in ADB *vs.* C, and 165 upregulated and 1002 downregulated genes in ADA *vs.* ADB. A core set of 251 genes was consistently altered by AD-MCI and modulated by VR-CRS. Functional enrichment highlighted the significant involvement of immune and inflammatory response pathways. Trend clustering pinpointed a key gene cluster (including transcription factors ZFP36, FOS, JUN, FOSB and the mitochondrial gene PMAIP1) that was upregulated in ADB and decreased to normal after VR-CRS. These genes showed significant correlations with immune cell proportions. Furthermore, widespread differential alternative splicing events were observed, affecting genes involved in cell cycle, immune response and neural function (e.g. AMPD2, MALAT1, DDX3X), which were also partially restored by VR-CRS treatment.
Conclusions: VR-CRS intervention is associated with transcriptomic changes in patients with AD-MCI, primarily involving modulation of immune and inflammatory pathways. It also appears to influence alternative splicing patterns. These preliminary findings provide novel molecular insights into the potential mechanisms of VR-CRS, suggesting it may act as a multi-faceted intervention targeting both transcriptional and post-transcriptional networks.

Keywords: Mild cognitive impairment, virtual reality-based cognitive rehabilitation software treatment, transcriptome, alternative splicing, immune and inflammatory responses.

INTRODUCTION

Mild Cognitive Impairment (MCI) represents an intermediate stage between normal ageing and dementia.[1] It is recognized as a critical transitional stage from the preclinical phase of Alzheimer's Disease (AD) to overt dementia.[2] AD, a prevalent neurodegenerative disorder and the leading form of dementia, accounts for approximately 60%–

Address correspondence to: Hongyan Li, MD, People's Hospital of Xinjiang Uygur Autonomous Region, Urumqi, Xinjiang, 830001, China. Email: lhyxxy@126.com

Date of Submission: 31 December 2025; Date of Acceptance: 18 February 2026

https://doi.org/10.54029/2026nfx

80% of all dementia cases[3], and has become the seventh leading cause of death globally.[4] Its core pathological features include extracellular deposition of β-amyloid (Aβ) forming senile plaques, intracellular neurofibrillary tangles resulting from by hyperphosphorylation of tau protein, accompanied by neuroinflammation, synaptic dysfunction and mitochondrial dysfunction, ultimately leading to synaptic loss and neurodegeneration.[5-8] At the MCI stage, Aβ plaques and tau tangles have already accumulated, yet significant neuronal loss is still preventable. With the intensification of global population aging, AD has emerged as a major public health concern threatening the health of the elderly.[9] Currently, there are no effective approaches to reverse or cure AD. Existing pharmacological treatments primarily include cholinesterase inhibitors (e.g. donepezil, rivastigmine and galantamine) and the NMDA receptor antagonist memantine. Although these medications can partially alleviate cognitive deficits and improve daily functioning, they are unable to halt disease progression.[10,11] Early intervention at this point—before the 'fire' of neurodegeneration has spread—offers the greatest chance to delay or even halt progression to dementia.[12]

Among non-pharmacological interventions, physical activity has been demonstrated as an effective strategy to slow the progression of AD. It not only helps maintain muscle function and physical agility, alleviate neurological and psychiatric symptoms, but also reduces medical dependence.[13] In addition, recreational physical activity in particular has been shown to positively influence cognitive performance.[14] In recent years, Virtual Reality (VR) technology—which integrates physical exercise with cognitive training—has emerged as an innovative non-pharmacological intervention, demonstrating potential value in the rehabilitation and cognitive training of AD patients.[15-17] Both immersive interventions using augmented reality glasses and non-immersive exergaming platforms have been reported to enhance cognitive and physical function in individuals with AD.[17,18] Moreover, studies indicate that VR-based relaxation scenarios can reduce anxiety and lower resting heart rate in patients with moderate AD.[19] Nevertheless, the specific molecular mechanisms underlying VR interventions in AD treatment, particularly their impact on gene expression and post-transcriptional regulation, remain to be systematically elucidated.

Advances in high-throughput sequencing have enabled transcriptomic analyses to provide novel insights into the molecular underpinnings of AD pathogenesis and progression.[20,21] RNA sequencing (RNA-seq) not only facilitates the identification of Differentially Expressed Genes (DEGs) but also enables the detection of Alternative Splicing Events (ASEs), thereby offering a comprehensive perspective on complex gene regulatory networks.[22-24]

In this study, we collected Peripheral Blood Mononuclear Cell (PBMC) samples from 12 participants, including healthy controls (Group C), AD patients before VR-based Cognitive Rehabilitation Software (VR-CRS) intervention (Group ADB) and AD-MCI patients after VR-CRS intervention (Group ADA). Using RNA-seq, we systematically investigated the effects of VR-CRS treatment on the transcriptomic profiles of AD-MCI patients. Our analysis focused on DEGs and differential alternative splicing events, supplemented by functional enrichment analysis, expression trend clustering, and co-expression network construction. The aim was to reveal dynamic changes in immune-related gene expression and splicing patterns in response to VR-CRS intervention. These findings are expected to provide new evidence for clarifying the molecular mechanisms of VR-CRS in AD-MCI treatment and to establish a theoretical foundation for advancing personalized therapeutic strategies for AD-MCI.

METHODS

Clinical assessment and sample preparation

Participants were inpatients diagnosed with AD-related MCI at the Department of Neurology, People's Hospital of Xinjiang Uygur Autonomous Region, and healthy residents from local communities between January 2023 and January 2024, who consented to participate and provided written informed consent. The study was approved by the Hospital's Medical Ethics Committee (Approval No.: KY2024052445). This study included 5 normal controls, 5 AD-related MCI patients pre-VR-CRS treatment, and 3 AD-related MCI patients post-VR-CRS treatment. VR-CRS primarily delivers orientation, attention, memory, visuospatial–executive, and calculation training through scenario modules of home-based task assignment and mall shopping. Among these, one ADA sample was paired with the ADB sample from

the same individual. The control group had a mean age of 60.5 ± 7.1 years (2 male, 3 female). The AD-related MCI patients had a mean age of 62.2 ± 8.4 years (pre-treatment: 2 male, 3 female; post-treatment: 1 male, 2 female). One patient withdrew from the study due to VR-induced dizziness, and another withdrew for personal reasons. No statistically significant differences ($P > 0.05$) were observed between the two groups of subjects before treatment regarding age, gender distribution, years of education, MoCA scores, MMSE scores, ADL scores, or scores on the individual sub-items of the MoCA scale.

The seven patients analyzed in this article were all individuals with AD-related MCI, confirmed to have AD biomarkers through examinations such as cerebrospinal fluid analysis or PET, while their daily living abilities remained largely intact. They had not received any cognitive-enhancing medication or other interventions prior to or during the study period. Hence, the experimental results can largely exclude the influence of drugs or other cognitive interventions. The immersive VR-based digital therapy was administered three times per week, each session lasting 20-30 minutes, over a continuous period of 8 weeks. During the project implementation phase, strict adherence to inclusion and exclusion criteria was maintained for subject selection, and the principle of randomization was followed. Diagnoses were verified by two senior neurologists. Cognitive scale assessments were administered by qualified assessors who had undergone consistent training. VR training was provided to rehabilitation therapists and participating physicians to ensure homogeneity in the delivery of the training.

MCI diagnostic criteria

In the diagnostic criteria for AD released by the National Institute on Aging-Alzheimer's Association (NIA-AA) working group in 2011, the diagnosis of amnestic Mild Cognitive Impairment (aMCI) due to AD was first proposed.[25] The clinical diagnostic criteria for MCI include: (1) cognitive impairment reported by the patient or an informant, or observed by a specialist; (2) objective evidence of impairment in one or more cognitive domains (assessed by neuropsychological evaluation), with episodic memory impairment being the most common; (3) mild impairment in complex instrumental activities of daily living, but essentially normal basic activities of daily living; (4) not meeting the diagnostic criteria for dementia

The expert consensus on Alzheimer's disease source mild cognitive impairment in China (2021)[26] recommends the following: (1) The diagnostic criteria for AD-MCI should adopt the NIA-AA diagnostic criteria (2011 and 2018) and IWG-2 (2014), with emphasis on the application of AD-related biological markers in the diagnosis of AD-MCI (Grade I recommendation, Grade A evidence); (2) When pathological, body fluid or molecular imaging (PET) biomarker detection cannot be carried out, identification can be made through clinical neuropsychological characteristics and imaging data, excluding other types of MCI (MCI related to Parkinson's disease, vascular disease, Lewy body disease, autoimmune encephalitis, etc.), and patients with MCI who meet the neuropsychological cognitive impairment characteristics of AD-MCI (such as hippocampal type amnestic syndrome) and cranial MRI imaging characteristics can be diagnosed as "AD-MCI" at the clinical level (expert consensus).

Inclusion criteria

Case Group (AD-related MCI): 1) Aged 50-80 years; 2) Met the 2011 NIA-AA or the 2021 Chinese Expert Consensus diagnostic criteria for AD-related MCI; 3) Native Mandarin or Uygur speaker; 4) Able to complete MRI, blood, and/or CSF tests; 5) Scored above the dementia threshold on MoCA and MMSE, had a CDR global score of 0.5, and an ADL score < 25 in this study.

Normal Control Group: 1) Aged 50-80 years; 2) No subjective cognitive complaints and no objective cognitive impairment; 3) Had normal MoCA and MMSE scores, a CDR global score of 0, and an ADL score of 20 in this study.

Exclusion criteria

Exclusion criteria for both groups included: 1) Advanced malignancy or severe/unstable systemic diseases affecting brain function or compliance with training; 2) Acute cerebrovascular events, active epilepsy, or history of psychiatric disorders; 3) Other identifiable causes of cognitive decline; 4) Significant hearing, visual, motor, or communication impairments hindering participation; 5) Unwillingness to participate or cooperate; 6) Use of cognition-enhancing or other specific psychoactive medications.

Specimen collection and intervention

Approximately 5 mL of peripheral blood was drawn from fasting participants into EDTA tubes in the morning and stored for subsequent isolation of Peripheral Blood Mononuclear Cells (PBMCs). VR group received immersive VR-based digital therapy. The VR-CRS intervention was administered 3 times per week, for 20-30 minutes per session, over 8 weeks.

RNA extraction and sequencing

Total RNA was extracted using TRIZOL (15596-018, Ambion, USA). The RNA was further purified with two phenol-chloroform treatments and then treated with RQ1 DNase (M6101, Promega, Madison, WI, USA) to remove DNA. The quality and quantity of the purified RNA were determined by measuring the absorbance at 260nm/280nm(A260/A280) using Ultrafine spectrophotometer (N50 touch, IMPLEN, Germany). The integrity of RNA was further verified by 1.0% agarose gel electrophoresis.

RNA-seq assay was performed by Wuhan Ruixing Biotec Co., Ltd (http://www.rxbio.cc). For each sample, 1 μg of total RNA was treated with RQ1 DNase (M6101，Promega，USA) to remove DNA before used for directional RNA-seq library preparation by VAHTS® Universal V8 RNA-seq Library Prep Kit for Illumina (NR605,Vazyme,China) for RNA-seq library preparation. The mRNAs were captured by VAHTS mRNA capture Beads (N401, Vazyme, China). Fragmented RNAs were converted into double strand cDNA. Following end repair and A tailing, the DNAs were ligated to VAHTS RNA Multiplex Oligos Set 1 for Illumina (N323, Vazyme, China), the ligated products were amplified，purified，quantified and stored at -80°C before sequencing. The strand marked with dUTP (the 2nd cDNA strand) is not amplified, allowing strand-specific sequencing.

For high-throughput sequencing, the libraries were prepared following the manufacturer's instructions and applied to Illumina NovaSeq Xplus system for 150 nt paired-end sequencing.

RNA-seq raw data clean and alignment

Raw reads containing more than 2-N bases were first discarded. Then adaptors and low-quality bases were trimmed from raw sequencing reads using FASTX-Toolkit (Version 0.0.13). The short reads less than 16nt were also dropped. The QC results were shown in Table S1. After that, clean reads were aligned to the gencode_GRCh38_v45 genome by HISAT2[27] allowing 4 mismatches. Uniquely mapped reads were used for gene reads number counting and FPKM calculation (fragments per kilobase of transcript per million fragments mapped).[28]

Differentially expressed genes (DEG) analysis

We used uniquely mapped reads for raw read count quantification at the gene level by HTSeq (version 2.0.2). Raw counts, but not FPKM values, were used for DESeq2[29] analysis, whereas FPKM was used only for visualization of gene expression. Benjamini-Hochberg (BH) false discovery rate (FDR) correction with adjusted P-value (FDR) < 0.05, combined with $|\log_2$fold change$| > 1$ as the cut-off for DEG identification.

Alternative splicing analysis

The Alternative Splicing Events (ASEs) and Regulated Alternative Splicing Events (RASEs) between the samples were defined and quantified by using the ABLas pipeline.[30,31] In brief, ABLas detection of ten types of ASEs was based on the splice junction reads, including exon skipping (ES), alternative 5' splice site(A5SS), alternative 3'splice site(A3SS), intron retention (IR), mutually exclusive exons (MXE), mutually exclusive 5'UTRs(5pMXE), mutually exclusive 3'UTRs (3pMXE), cassette exon, A3SS&ES and A5SS&ES. For sample pair comparison, Fisher's exact test was selected to determine statistical significance, using the alternative reads and model reads of the samples as input data. We calculated the changed ratio of alternatively spliced reads and constitutively spliced reads between compared samples, which was defined as the RASE ratio. The RASE ratio >=0.2 and *p*-value <= 0.05 were set as the threshold for RASEs detection. For repetition comparison, Student's t-test was performed to evaluate the significance of the ratio alteration of AS events. Those events which were significant at *P*-value cutoff of 0.05 were considered non intron retention (NIR) RASEs.

Functional enrichment analysis

To sort out functional categories of DEGs, Gene Ontology (GO) terms and KEGG pathways were identified using KOBAS 2.0 server.[32] Hyper geometric test and Benjamini-Hochberg FDR controlling procedure were used to define the enrichment of each term.

Cell-type quantification

The CIBERSORT algorithm (v1.03)[33] was used with the default parameter for estimating immune cell fractions using TPM values of each expressed gene. A total of 22 human immune cell phenotypes can be deconstructed by CIBERSORT, including seven T cell types [CD8 T cells, naïve CD4 T cells, memory CD4 resting T cells, memory CD4 activated T cells, T follicular helper cells, and regulatory T cells (Tregs)]; naïve and memory B cells; plasma cells; resting and activated NK cells; monocytes; macrophages M0, M1, and M2; resting and activated dendritic cells; resting and activated mast cells; eosinophils; and neutrophils. An R package, Immunedeconv (v2.0.2)[34], that provided a unified interface to seven deconvolution methods was used for estimating immune cell fractions, while CIBERSORT algorithm was applied for estimating immune cell fractions.

Co expression analysis

Co-expression analysis was performed for all differentially expressed RBPs (DERBPs) and DASEs. Meanwhile, Pearson correlation coefficient between DERBPs and DASEs was calculated, and DERBP-DASE relationship pairs satisfying absolute value of correlation coefficient ≥ 0.8 and P value < 0.05 were screened.

Statistical analysis

All statistical analyses were performed using R software. P-value <0.05 was used as the significance criterion.

RESULTS

Transcriptome analysis of differentially expressed genes among ADB, ADA and C groups

To investigate the molecular mechanisms underlying VR-CRS intervention in AD-MCI, we conducted transcriptome sequencing (RNA-seq) on peripheral blood samples from healthy volunteers (Group C, N=5), AD-MCI patients before VR therapy (Group ADB, N=5) and AD-MCI patients after VR-CRS treatment (Group ADA, N=3). No statistically significant differences were observed between the two groups before treatment in terms of age, gender distribution, years of education, MoCA scores, MMSE scores, ADL scores, or scores on the individual sub-items of the MoCA scale ($P > 0.05$). Principal component analysis revealed a clear shift in the gene expression profile of the ADA group compared to the ADB group (Figure 1A). Analysis of differentially expressed genes (DEGs) showed that, relative to Group C, Group ADB exhibited 421 up-regulated and 186 down-regulated genes. In contrast, comparison between Group ADA and Group ADB identified 165 up-regulated and 1002 down-regulated genes (Figure 1B). Overlap analysis further indicated that 251 genes were consistently differentially expressed both before and after VR-CRS intervention (Figure 1C). Among these, 229 genes were upregulated in AD-MCI but downregulated following VR-CRS treatment, while 22 genes were downregulated in AD-MCI and upregulated after treatment. GO functional enrichment analysis demonstrated that in the ADB *vs.* C comparison, up-regulated genes were primarily associated with pathways such as inflammatory response, while down-regulated genes were enriched in chemokine-mediated signaling, inflammatory response and adaptive immune response. In the ADA *vs.* ADB comparison, up-regulated DEGs were mainly involved in immune and inflammatory responses, whereas down-regulated DEGs were related to inflammatory response and endoplasmic reticulum stress response (Figure 1D). These findings suggest that VR-CRS therapy may ameliorate cognitive impairment associated with AD-MCI by modulating the expression of genes implicated in inflammatory processes.

Dynamic analysis of DEGs associated with healthy population, before and after VR-CRS for AD-MCI

To identify key regulatory genes involved in VR-CRS therapy for AD-MCI, we performed K-means clustering on DEGs, resulting in nine functional clusters (clusters 1–9). Cluster 4 was of particular interest, as the expression trends of its DEGs were similar between the ADA and C groups but up-regulated in the ADB group, indicating a potential association with the therapeutic effect of VR-CRS (Figure 2A). GO enrichment analysis of DEGs in cluster 4 revealed significant involvement in processes such as nucleosome assembly, negative and positive regulation of transcription by RNA polymerase II, heterochromatin formation and immune response (Figure 2B). From the top 30 genes in this cluster, we identified five AD-associated genes—ZFP36, FOS, JUN, FOSB and PMAIP1—all of which were significantly up-regulated in AD-MCI patients and markedly

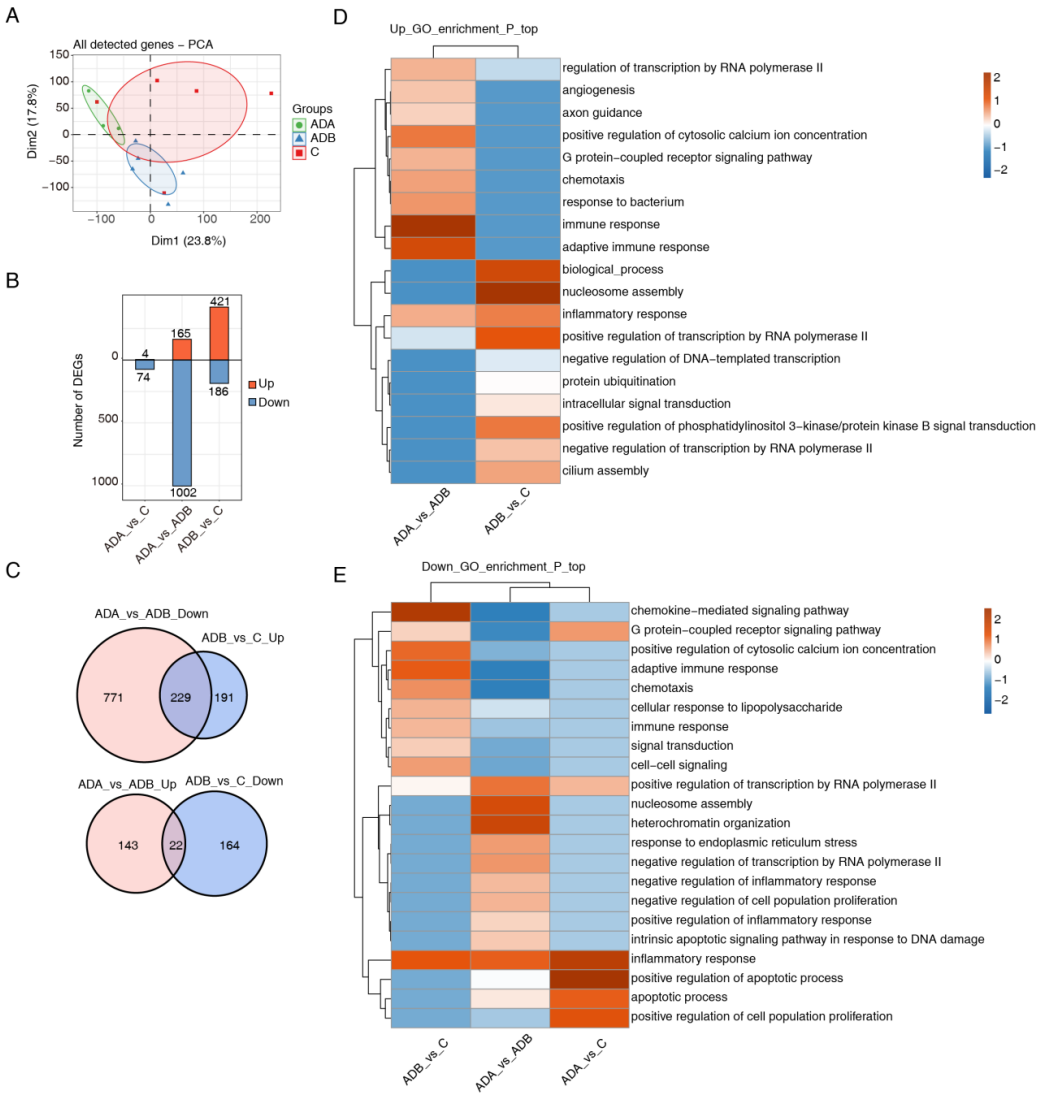

Figure 1. Transcriptomic profiling of differentially expressed genes in AD-MCI patients undergoing VR-CRS therapy

(A) Principal component analysis (PCA) of samples after normalizing all genes expression levels. The ellipse for each group is the confidence ellipse.

(B) Bar plot showing the numbers of up-regulated DEGs and down-regulated DEGs.

(C) Venn diagram shows the overlapped DEGs between different comparison groups (ADA vs. ADB, ADB vs. C and ADA vs. C).

(D) GO biological process results obtained by up-regulated genes in each comparison group.

(E) GO biological process results obtained by down-regulated genes in each comparison group.

down-regulated following VR-CRS therapy (Figure 2C). To further investigate the immune interactions, we employed the CIBERSORT algorithm (v1.03) to deconvolute the immune cell infiltration. This analysis revealed that PMAIP1 expression was negatively correlated with regulatory T cells and monocytes and positively correlated with neutrophils. Similarly, ZFP36 was negatively correlated with regulatory T cells and monocytes, while FOS showed negative correlations with Tregs, activated NK cells and monocytes and a positive correlation

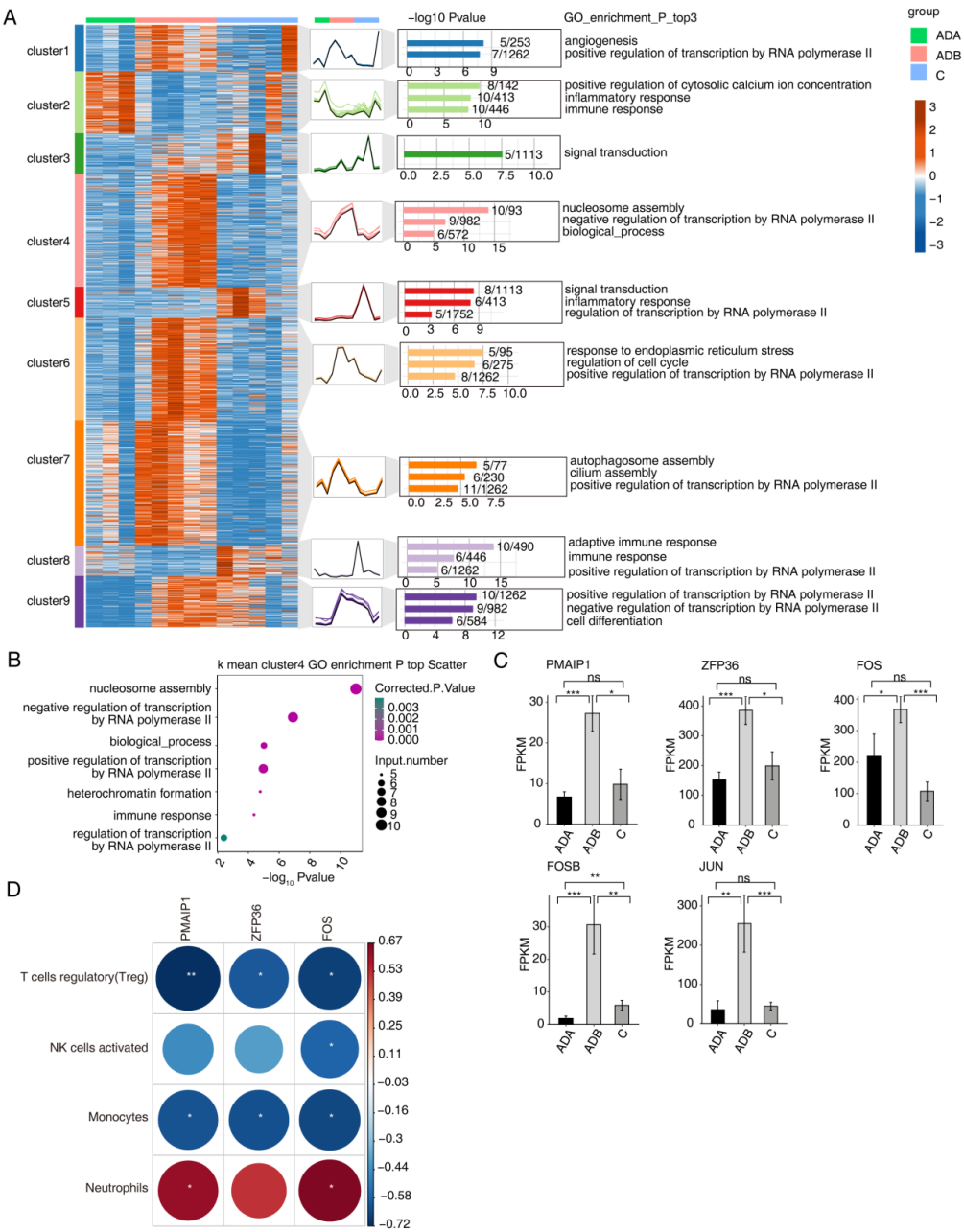

Figure 2. Dynamic expression patterns and functional analysis of DEGs in VR-CRS therapy for AD-MCI.

(A) Heatmap and line chart displayed the cluster analysis of the all DEGs from different comparison groups base on K-means, and exhibiting the top3 enriched GO BP terms in each cluster.

(B) Scatter plot exhibiting the most enriched GO biological process results of DEGs in cluster4 base on K-means.

(C) The schematic diagrams depict the result of some important DEGs. Error bars represent mean ± SEM. *** P-value < 0.001.** P-value < 0.01.* P-value < 0.05.

(D) The dot-plot demonstrated the correlations between each immune microenvironment infiltration cell type and each gene. Different color indicates correlation of immunocyte-gene regulator and the size of the point indicates the degree of significance. Significant ones were labeled with star. *P <=0.05; **P <= 0.01; *** P <= 0.001.

with neutrophils (Figure 2D). Notably, ZFP36, FOS, JUN and FOSB are transcription factors, suggesting that VR-CRS therapy may restore dysregulated transcriptional networks, leading to downstream feedback regulation—particularly of immune-related target genes—that contributes to therapeutic benefits.

Dynamic analysis of alternative splicing genes (ASGs) in three groups

Beyond DEGs, we identified a substantial number of DASEs (Figure 3A). Among them, Intron Retention (IntronR), Alternative 5' Splice Site (A5SS) and Alternative 3' Splice Site (A3SS) events were the most prevalent types (Figure 3B). Genes subject to DASEs mostly contained 1-2 DASEs (Figure 3C). Gene Ontology (GO) enrichment analysis of DASE genes (DASGs) revealed distinct functional profiles. In the ADB *vs.* C comparison, these DASGs were primarily associated with the regulation of the cell cycle, RNA splicing, defense response to virus, peptidyl-serine autophosphorylation, cellular response to hydrogen peroxide, chromatin remodeling, mRNA processing, regulation of RNA splicing, and regulation of apoptosis (Figure 3D). In the ADA *vs.* ADB comparison, enrichment was observed for the regulation of the cell cycle, negative regulation of NF-κB activity, protein import into the nucleus, cellular response to hydrogen peroxide, T cell receptor signaling pathway, apoptosis, cellular senescence, peptidyl-serine phosphorylation, positive regulation of interferon-beta production, etc. (Figure 3D).

K-means clustering of the splicing ratio values for DASEs defined nine distinct clusters. Notably, the expression patterns of DASEs in cluster 2 and cluster 8 showed similar levels in the ADA and C groups but were upregulated and downregulated in the ADB group, respectively. This pattern suggests a potential link to the VR-CRS intervention effect (Figure 3E and Figure S1). GO enrichment analysis of these two clusters highlighted pathways including regulation of the cell cycle, signal transduction, nervous system development, regulation of apoptosis, defense response to virus, innate immune response, spermatogenesis, positive regulation of transcription by RNA polymerase II, cell differentiation, and regulation of transcription by RNA polymerase II (Figure 3F). From these clusters, we identified six key genes associated with neurological diseases: AMPD2, EIF1, MALAT1, DDX3X, SRSF3 and RPL41. The alternative splicing ratio for AMPD2, EIF1, MALAT1 and DDX3X was elevated in the ADB group and returned to baseline levels after VR-CRS therapy (Figure 3G). Conversely, the alternative splicing ratio for SRSF3 and RPL41 was reduced in the ADB group and increased significantly in the ADA group (Figure 3G).Taken together, we identified six neurologically relevant genes whose splicing patterns are significantly altered by the disease and subsequently modulated by VR-CRS intervention, suggesting their potential role in mediating the therapeutic effects of VR-CRS in the recovery process.

Network between differential RBPs and ASGs

Given that alternative splicing is frequently regulated by RNA-binding proteins (RBPs), we performed a co-expression analysis (|correlation coefficient| $\geq$ 0.8 and $P < 0.05$) between the ASGs in clusters 2 and 8 and the differentially expressed RBPs (DERBPs) identified in this study. The resulting co-expressed gene networks were predominantly enriched in pathways such as innate immune response, defense response to virus, regulation of the cell cycle, apoptotic process and signal transduction (Figure 4A). The expression patterns of the relevant RBPs across samples were displayed in Figure 4B. Specifically, RBPs that were upregulated in the ADB group were downregulated in both C and ADA groups, reinforcing their potential regulatory role in the VR-CRS therapeutic process.

DISCUSSION

AD is a multifactorial neurodegenerative disorder characterized by progressive cognitive decline.[35,36] The AD-MCI is now understood not merely as a transitional phase between normal aging and dementia, but as a clinically identifiable window in which key pathologies such as Aβ plaques and tau tangles are already present, yet substantial neurodegeneration may still be modifiable.[12] It is within this critical therapeutic window that early non-pharmacological interventions hold promise for slowing or altering disease trajectory. VR has thus emerged as a candidate intervention[15], yet its molecular mechanisms of action in AD-MCI remain largely unexplored.

Therefore, this study employed RNA-seq of PBMCs to systematically investigate the transcriptomic effects of VR-CRS in

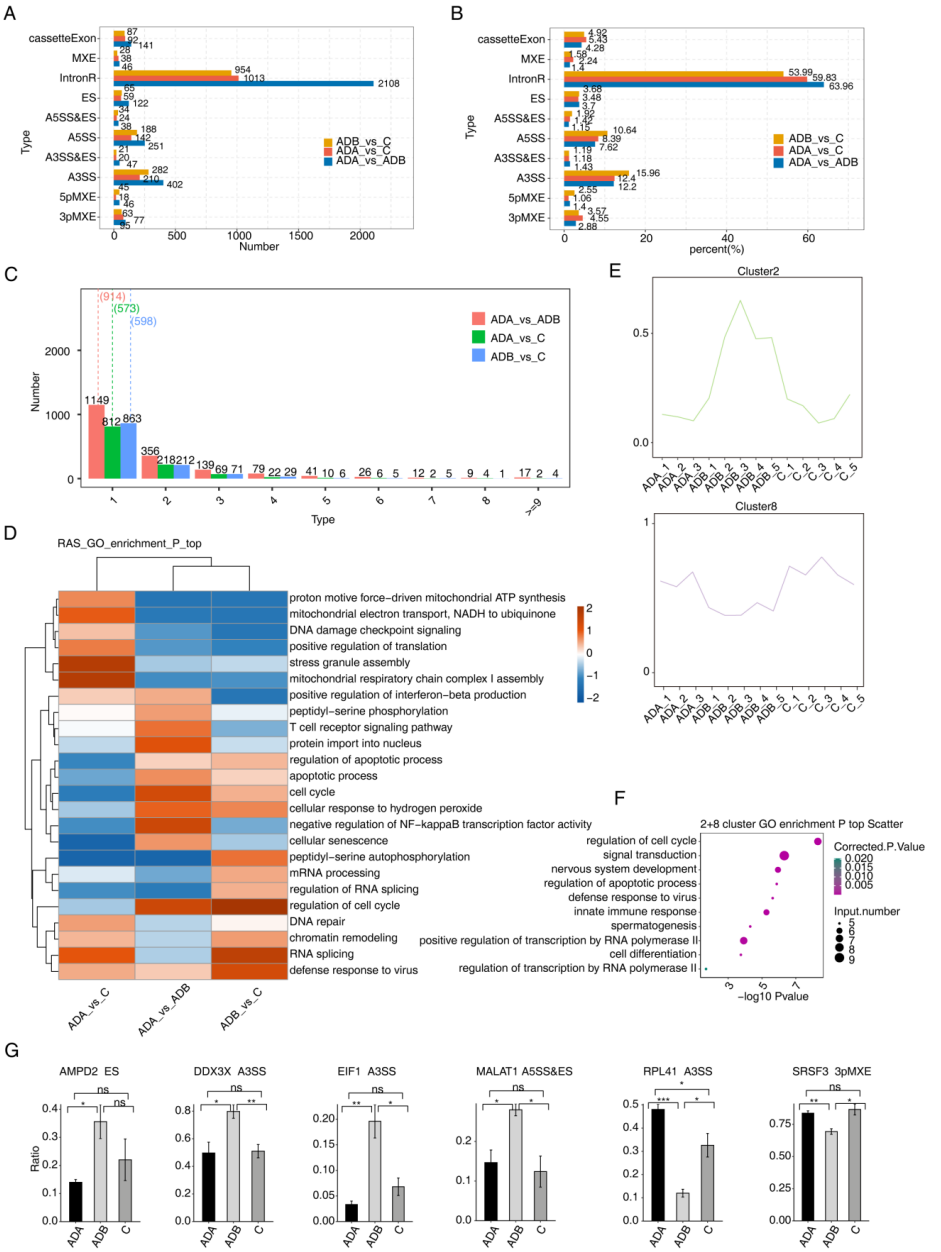

Figure 3. Analysis of alternative splicing events (ASEs) and their functional implications in VR-CRS therapy for AD-MCI.

(A) Bar plot showing the number of each type alternative splicing event (ASE) in each comparison groups.

(B) Bar plot showing the percentages of each type ASE in each comparison groups.

(C) The bar chart displays the number of genes with different occurrences of ASE (in ascending order of ASE occurrence), with the median marked by dashed lines. Mark X and Y in parentheses. Y: Position of values in ASE. X: The number of occurrences of ASE.

(D) GO biological process results obtained by alternative splicing genes (ASGs) in each comparison group.

(E) The line chart displays the clustering analysis of all ASGs for different comparison groups based on K-means. The diagram shows cluster2 and cluster8.

(F) Scatter plot exhibiting the most enriched GO biological process results of alternative splicing genes (ASGs) in cluster2 and cluster8 base on K-means.

(G) The schematic diagrams depict the result of alternative splicing genes. Error bars represent mean ± SEM. *** P-value < 0.001.** P-value < 0.01.* P-value < 0.05

The schematic diagrams depict the result of alternative splicing genes. Error bars represent mean ± SEM. *** P-value < 0.001. ** P-value < 0.01.* P-value < 0.05

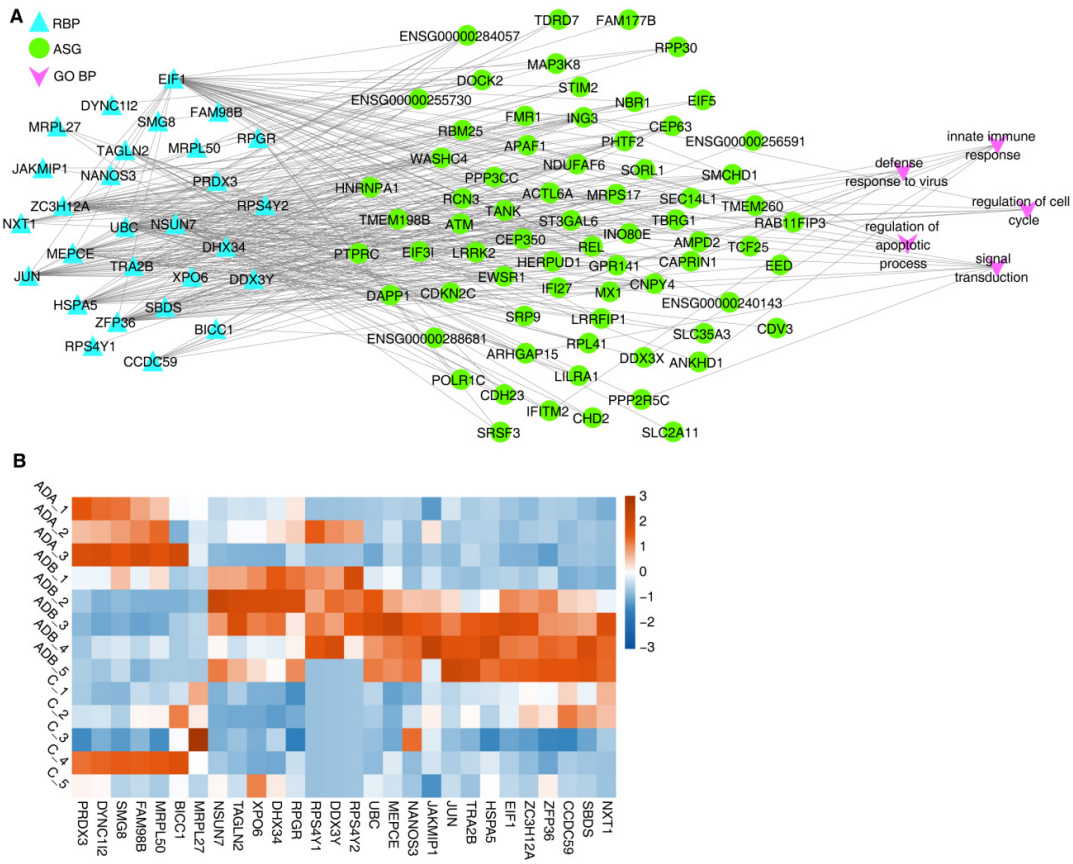

Figure 4. Interaction network of differential RNA-binding proteins and alternative splicing genes in VR-CRS therapy for AD-MCI.
(A) Network diagram showing RBP-ASGs (from clusters 2 and cluster8 base on K-means) relationship.
(B) Heat map showing expression levels of RBPs

patients with AD-MCI. Prior to analyzing these molecular changes, we confirmed that enrolled AD-MCI patients and healthy controls were well-matched in age, sex, and baseline cognitive scores (MoCA, MMSE, CDR, ADL; all $p>0.05$). Among the AD-MCI cohort, the two participants who withdrew (one due to VR-induced dizziness, another for personal reasons) showed no significant differences in these baseline characteristics compared to completers, although this comparison was limited by the small number of dropouts. This suggests that the subsequent molecular findings are unlikely to be confounded by systematic baseline disparities or selective attrition.

In recent years, mounting evidence suggests that neuroinflammation occurs early in AD pathogenesis, even before detectable histopathological degeneration, making it a promising therapeutic target.[37-39] Our initial analysis of DEGs revealed widespread activation of inflammatory and immune response pathways in AD patients (ADB group) compared to healthy controls. Following VR-CRS intervention (ADA group), the expression levels of many immune- and inflammation-related genes were significantly restored. This strongly implies that modulation of systemic and neuroinflammatory immune status may represent a core mechanism through which VR-CRS exerts neuroprotective and cognitive-enhancing effects. Furthermore, trend cluster analysis identified a set of key genes—including ZFP36, FOS, JUN, FOSB and PMAIP1—whose expression normalized post-VR-CRS. ZFP36, an RBP and transcription factor (TF), is upregulated in AD and has been identified as a shared biomarker in AD and chronic kidney disease.[40,41] FOS is an important TF found in the hippocampal region of AD, where the density of FOS-positive neuronal

outlines increases. Inhibiting the ERK-FOS signaling axis can alleviate neuroinflammation and reverse AD pathological symptoms.[42,43] JUN is another TF observed in tau neurofibrillary tangles. Inhibiting c-Jun N-terminal kinase (JNK), which activates JUN, can block APP/Aβ-induced neurodegeneration and exert neuroprotective effects.[44,45] The FOSB gene belongs to the FOS TF gene family. ΔFosB is a truncated splice variant of the FosB protein, found to be increased in the hippocampus of AD mice, and inhibiting ΔFosB activity can improve cognitive ability in AD mice.[46,47] PMAIP1, a mitochondrial metabolism-related gene markedly upregulated in AD, may promote disease progression by impairing mitochondrial function in hippocampal neurons.[48] Most of these genes are immediate-early genes or TFs involved in proliferation, apoptosis and immune regulation. Their elevated expression in AD was markedly suppressed by VR-CRS intervention, and these changes correlated with shifts in immune cell subsets such as regulatory T cells and monocytes. This suggests that VR-CRS may help normalize a dysregulated TF network in AD-MCI, leading to broad corrective effects on downstream immune-related gene expression and ultimately mitigating disease progression.

Alternative splicing and its regulatory factors, RBPs, are increasingly recognized as key players in human disease, with growing research focusing on the role of post-transcriptional regulation in pathogenesis.[49,50] Deep proteomic network analyses have revealed widespread RBP and AS dysregulation in AD[51], and RNA-based therapies targeting splicing events offer new hope for treatment.[52,53] In this study, we report for the first time in the context of VR-CRS intervention for AD-MCI the presence of extensive Differential Alternative Splicing Events (DASE) across the transcriptome. Genes involved in DASEs were enriched in pathways related to cell cycle regulation, stress response, innate immunity and T cell receptor signaling. Importantly, we observed disrupted splicing patterns in several nervous system-related genes—including AMPD2, MALAT1, DDX3X, and SRSF3—in AD patients, which showed a restorative trend after VR-CRS intervention. DDX3X, an ATP-dependent RNA helicase of the DEAD-box family, has been shown through interpretable machine learning to accurately predict AD progression.[54] AMPD2, a key enzyme highly expressed in neural and muscle tissues, shows elevated expression and activity in AD.[55,56] MALAT1, a long non-coding RNA downregulated in AD plasma and inversely correlated with inflammatory mediators such as PTGS2[57], promotes neuronal recovery via the miR-30b/CNR1 network and PI3K/AKT pathway.[58] RPL41 and SRSF3 also demonstrate abnormal expression in AD.[59-61] These findings suggest that dysregulated splicing of these genes may be a previously overlooked aspect of AD-MCI pathogenesis, and that VR-CRS may partially rescue this dysregulation by restoring RBP function or expression. Our co-expression analysis between DASGs and DERBPs offers preliminary support for this hypothesis.

Given the exploratory nature of this study, several important limitations warrant consideration. First, the small sample size may limit the statistical power and generalizability of our findings, underscoring the need for validation in larger independent cohorts. Second, our analysis relied on PBMCs, and it remains unclear whether the observed transcriptomic changes fully mirror those occurring in the central nervous system. Future studies integrating cerebrospinal fluid biomarkers or neuroimaging data would help bridge this peripheral–central gap. Most notably, this study did not include longitudinal clinical cognitive assessments (e.g. serial MoCA/MMSE scores) that could be directly correlated with the molecular alterations identified here. Consequently, while the observed transcriptomic shifts are suggestive of a biological response to VR-CRS intervention, they cannot be interpreted as direct evidence of clinical efficacy. Finally, the functional implications of the key candidate genes and splicing events reported here were derived from bioinformatic analyses. Experimental validation in cellular or animal models is therefore essential to establish causal mechanistic links.

Therefore, future studies with larger, independent cohorts are essential to validate the identified transcriptomic and alternative splicing signatures. Additionally, since our analysis was based on peripheral blood mononuclear cells (PBMCs), it remains to be determined whether these molecular changes fully reflect those within the central nervous system. Subsequent research would be strengthened by correlating these peripheral biomarkers with cerebrospinal fluid profiles or neuroimaging data to bridge the peripheral-central gap. Crucially, this study lacked direct clinical cognitive outcome measures (e.g. changes in MoCA or MMSE scores post-intervention) correlated with the

molecular changes. Therefore, the observed transcriptomic shifts, while promising, cannot be directly equated with therapeutic efficacy at the clinical level.

In conclusion, this study provides preliminary transcriptomic evidence linking VR-CRS intervention to molecular reprogramming in AD-MCI patients. Our analysis identified three key layers of response: 1) normalization of immune-inflammatory transcriptional networks; 2) restoration of dysregulated immediate-early genes (ZFP36, FOS, JUN, FOSB) and mitochondrial regulator PMAIP1 toward healthy control patterns; and 3) modulation of alternative splicing in neural-unction-associated genes. These multi-level molecular shifts suggest that VR-CRS may act through coordinated transcriptional and post-transcriptional mechanisms.

The current findings establish an initial molecular framework for understanding how non-pharmacological cognitive rehabilitation engages biological pathways relevant to early AD progression. Future validation studies should focus on correlating these molecular signatures with longitudinal cognitive trajectories and neuroimaging biomarkers to assess their potential utility as predictive or monitoring indicators in larger, controlled trials.

DISCLOSURE

Data availability: The datasets generated during the current study are available from the corresponding author on reasonable request.

Financial support: This work was supported by the "Tianshan Talents Program for High-Level Medical and Health Professionals: Special Research Project for Young Medical Science and Technology Talents in Health and Wellness(TSYC202301B131).

Conflicts of interest: None

REFERENCES

1. Ruiz-Vanoye JA, Díaz-Parra O, Márquez-Vera MA, et al. Symmetry in genetic distance metrics: Quantifying variability in neurological disorders for personalized treatment of Alzheimer's and dementia. Symmetry 2025;17:172. https://doi.org/10.3390/sym17020172
2. Mian M, Tahiri J, Eldin R, Altabaa M, Sehar U, Reddy PH. Overlooked cases of mild cognitive impairment: Implications to early Alzheimer's disease. Ageing Res Rev 2024;98:102335. https://doi.org/10.1016/j.arr.2024.102335
3. 2024 Alzheimer's disease facts and figures. Alzheimers Dement 2024;20:3708-821. https://doi.org/10.1002/alz.13809
4. 2025 Alzheimer's disease facts and figures. Alzheimers Dement 2025;21: https://doi.org/10.1002/alz.70235
5. Long JM, Holtzman DM. Alzheimer disease: An update on pathobiology and treatment strategies. Cell 2019;179:312-39. https://doi.org/10.1016/j.cell.2019.09.001
6. Jia J, Ning Y, Chen M, et al. Biomarker changes during 20 years preceding Alzheimer's disease. N Engl J Med 2024;390:712-22. https://doi.org/10.1056/NEJMoa2310168
7. Abdelnour C, Agosta F, Bozzali M, et al. Perspectives and challenges in patient stratification in Alzheimer's disease. Alzheimers Res Ther 2022;14:112. https://doi.org/10.1186/s13195-022-01055-y
8. D'Alessandro MCB, Kanaan S, Geller M, Praticò D, Daher JPL. Mitochondrial dysfunction in Alzheimer's disease. Ageing Res Rev 2025;107:102713. https://doi.org/10.1016/j.arr.2025.102713
9. Korczyn AD, Grinberg LT. Is Alzheimer disease a disease? Nat Rev Neurol 2024;20:245-51. https://doi.org/10.1038/s41582-024-00940-4
10. Zheng Q, Wang X. Alzheimer's disease: insights into pathology, molecular mechanisms, and therapy. *Protein Cell* 2025;16:83-120. https://doi.org/10.1093/procel/pwae026
11. Frisoni GB, Aho E, Brayne C, *et al.* Alzheimer's disease outlook: controversies and future directions. *Lancet* 2025;406:1424-42. https://doi.org/10.1016/s0140-6736(25)01389-3
12. Choi MS. Is it possible-to-prevent-progression-from-mci-to-alzheimer-disease. *Neurol Curr Res* 2018;1(1):1002. https://doi.org/10.3390/sym17020172
13. Stella F, Canonici AP, Gobbi S, Galduroz RF, Cação Jde C, Gobbi LT. Attenuation of neuropsychiatric symptoms and caregiver burden in Alzheimer's disease by motor intervention: a controlled trial. *Clinics (Sao Paulo)* 2011;66:1353-60. https://doi.org/10.1590/s1807-59322011000800008
14. Dregan A, Gulliford MC. Leisure-time physical activity over the life course and cognitive functioning in late mid-adult years: a cohort-based investigation. *Psychol Med* 2013;43:2447-58. https://doi.org/10.1017/s0033291713000305
15. Santos VD, Costa AC, Junior NC, Delaere FJ, Serlet S, Dourado MCN. Virtual reality interventions and their effects on the cognition of individuals with Alzheimer's disease: A systematic review and meta-analysis. *J Alzheimers Dis* 2025;103:68-80. https://doi.org/10.1177/13872877241299037
16. Doniger GM, Beeri MS, Bahar-Fuchs A, *et al*. Virtual reality-based cognitive-motor training for middle-aged adults at high Alzheimer's disease risk: A randomized controlled trial. *Alzheimers Dement* 2018;4:118-29. https://doi.org/10.1016/j.trci.2018.02.005
17. Vásquez-Carrasco E, Huenchuquen C, Ferrón C, *et al*. Effectiveness of leisure-focused occupational therapy interventions in middle-aged and older

people with mild cognitive impairment: A systematic review. *Healthcare (Basel)*. 2024;12(24): 2521. https://doi.org/10.3390/healthcare12242521
18. Yi Y, Hu Y, Cui M, Wang C, Wang J. Effect of virtual reality exercise on interventions for patients with Alzheimer's disease: A systematic review. *Front Psychiatry* 2022;13:1062162. https://doi.org/10.3389/fpsyt.2022.1062162
19. Sánchez-Nieto D, Castaño-Castaño S, Navarro-Martos R, Obrero-Gaitán E, Cortés-Pérez I, Nieto-Escamez F. An intervention on anxiety symptoms in moderate Alzheimer's disease through virtual reality: A feasibility study and lessons learned. *Int J Environ Res Public Health* 2023;20(3):2727. https://doi.org/10.3390/ijerph20032727
20. Xia LY, Tang L, Huang H, Luo J. Identification of potential driver genes and pathways based on transcriptomics data in Alzheimer's disease. *Front Aging Neurosci* 2022;14:752858. https://doi.org/10.3389/fnagi.2022.752858
21. Rybak-Wolf A, Plass M. RNA dynamics in Alzheimer's disease. *Molecules (Basel)* 2021;26: https://doi.org/10.3390/molecules26175113
22. Conesa A, Madrigal P, Tarazona S, *et al*. A survey of best practices for RNA-seq data analysis. *Genome Biol* 2016;17:13. https://doi.org/10.1186/s13059-016-0881-8
23. Li J, Varghese RS, Ressom HW. RNA-seq data analysis. *Methods Mol Biol* 2024;2822:263-90. https://doi.org/10.1007/978-1-0716-3918-4_18
24. Wang Y, Xie Z, Kutschera E, Adams JI, Kadash-Edmondson KE, Xing Y. rMATS-turbo: an efficient and flexible computational tool for alternative splicing analysis of large-scale RNA-seq data. *Nat Protoc* 2024;19:1083-104. https://doi.org/10.1038/s41596-023-00944-2
25. Sperling RA, Aisen PS, Beckett LA, *et al.* Toward defining the preclinical stages of Alzheimer's disease: recommendations from the National Institute on Aging-Alzheimer's Association workgroups on diagnostic guidelines for Alzheimer's disease. *Alzheimers Dement* 2011;7:280-92. https://doi.org/10.1016/j.jalz.2011.03.003
26. Dementia and Cognitive Impairment Group of the Neurology Branch of the Chinese Medical Association. Chinese expert consensus on the diagnosis and treatment of mild cognitive impairment due to Alzheimer's disease 2021. *Chin J Neurol* 2022;55:421-40. https://doi.org/10.3760/cma.j.cn113694-20211004-00679
27. Kim D, Langmead B, Salzberg SL. HISAT: a fast spliced aligner with low memory requirements. *Nat Methods* 2015;12:357-60. https://doi.org/10.1038/nmeth.3317
28. Trapnell C, Williams BA, Pertea G, *et al.* Transcript assembly and quantification by RNA-Seq reveals unannotated transcripts and isoform switching during cell differentiation. *Nat Biotechnol* 2010;28:511-5. https://doi.org/10.1038/nbt.1621
29. Love MI, Huber W, Anders S. Moderated estimation of fold change and dispersion for RNA-seq data with DESeq2. *Genome Biol* 2014;15:1-21. https://doi.org/10.1186/s13059-014-0550-8
30. Jin L, Li G, Yu D, *et al.* Transcriptome analysis reveals the complexity of alternative splicing regulation in the fungus Verticillium dahliae. *BMC Genomics* 2017;18(1):130. https://doi.org/10.1186/s12864-017-3507-y
31. Xia H, Chen D, Wu Q, *et al.* CELF1 preferentially binds to exon-intron boundary and regulates alternative splicing in HeLa cells. *Biochim Biophys Acta Gene Regul Mech* 2017;1860:911-21. https://doi.org/10.1016/j.bbagrm.2017.07.004
32. Xie C, Mao X, Huang J, *et al.* KOBAS 2.0: a web server for annotation and identification of enriched pathways and diseases. *Nucleic Acids Res* 2011;39:W316-W22. https://doi.org/10.1093/nar/gkr483
33. Newman AM, Liu CL, Green MR, *et al.* Robust enumeration of cell subsets from tissue expression profiles. *Nat Methods* 2015;12:453-7. https://doi.org/10.1007/978-1-0716-0327-7_16
34. Sturm G, Finotello F, List M. Immunedeconv: An R package for unified access to computational methods for estimating immune cell fractions from bulk RNA-sequencing data. *Methods Mol Biol* 2020;2120:223-32. https://doi.org/10.1007/978-1-0716-0327-7_16
35. Valiukas Z, Ephraim R, Tangalakis K, Davidson M, Apostolopoulos V, Feehan J. Immunotherapies for Alzheimer's disease-A review. *Vaccines* 2022;10: https://doi.org/10.3390/vaccines10091527
36. Wilson DM, 3rd, Cookson MR, Van Den Bosch L, Zetterberg H, Holtzman DM, Dewachter I. Hallmarks of neurodegenerative diseases. *Cell* 2023;186:693-714. https://doi.org/10.1016/j.cell.2022.12.032
37. Botella Lucena P, Heneka MT. Inflammatory aspects of Alzheimer's disease. *Acta Neuropathol* 2024;148:31. https://doi.org/10.1007/s00401-024-02790-2
38. Han J, Zhang Z, Zhang P, *et al*. The roles of microglia and astrocytes in neuroinflammation of Alzheimer's disease. *Front Neurosci* 2025;19:1575453. https://doi.org/10.3389/fnins.2025.1575453
39. Heneka MT, Carson MJ, El Khoury J, *et al*. Neuroinflammation in Alzheimer's disease. *Lancet Neurol* 2015;14:388-405. https://doi.org/10.1016/s1474-4422(15)70016-5
40. Shippy DC, Ulland TK. Exploring the zinc-related transcriptional landscape in Alzheimer's disease. *IBRO Neurosci Rep* 2022;13:31-7. https://doi.org/10.1016/j.ibneur.2022.06.002
41. Li J, Li Y, Niu J, Zhang J, Cheng X. Exploration of the shared genetic biomarkers in Alzheimer's disease and chronic kidney disease using integrated bioinformatics analysis. *Medicine* 2023;102:e35555. https://doi.org/10.1097/md.0000000000035555
42. Wang C, Cui X, Dong Z, *et al.* Attenuated memory impairment and neuroinflammation in Alzheimer's disease by aucubin via the inhibition of ERK-FOS axis. *Int Immunopharmacol* 2024;126:111312. https://doi.org/10.1016/j.intimp.2023.111312
43. Marcus DL, Strafaci JA, Miller DC, *et al.* Quantitative neuronal c-fos and c-jun expression in Alzheimer's disease. *Neurobiol Aging* 1998;19:393-400. https://doi.org/10.1016/s0197-4580(98)00077-3
44. Pearson AG, Byrne UT, MacGibbon GA, Faull

RL, Dragunow M. Activated c-Jun is present in neurofibrillary tangles in Alzheimer's disease brains. *Neurosci Lett* 2006;398:246-50. https://doi.org/10.1016/j.neulet.2006.01.031
45. Braithwaite SP, Schmid RS, He DN, *et al*. Inhibition of c-Jun kinase provides neuroprotection in a model of Alzheimer's disease. *Neurobiol Dis* 2010;39:311-7. https://doi.org/10.1016/j.nbd.2010.04.015
46. Corbett BF, You JC, Zhang X, *et al.* ΔFosB regulates gene expression and cognitive dysfunction in a mouse model of Alzheimer's disease. *Cell Rep* 2017;20:344-55. https://doi.org/10.1016/j.celrep.2017.06.040
47. You JC, Stephens GS, Fu CH, Zhang X, Liu Y, Chin J. Genome-wide profiling reveals functional diversification of ΔFosB gene targets in the hippocampus of an Alzheimer's disease mouse model. *PLoS One* 2018;13:e0192508. https://doi.org/10.1371/journal.pone.0192508
48. Ling Y, Hu L, Chen J, Zhao M, Dai X. The mechanism of mitochondrial metabolic gene PMAIP1 involved in Alzheimer's disease process based on bioinformatics analysis and experimental validation. *Clinics (Sao Paulo)* 2024;79:100373. https://doi.org/10.1016/j.clinsp.2024.100373
49. Scotti MM, Swanson MS. RNA mis-splicing in disease. *Nat Rev Genet* 2016;17:19-32. https://doi.org/10.1038/nrg.2015.3
50. Tao Y, Zhang Q, Wang H, Yang X, Mu H. Alternative splicing and related RNA binding proteins in human health and disease. *Signal Transduct Target Ther* 2024;9:26. https://doi.org/10.1038/s41392-024-01734-2
51. Johnson ECB, Dammer EB, Duong DM, *et al*. Deep proteomic network analysis of Alzheimer's disease brain reveals alterations in RNA binding proteins and RNA splicing associated with disease. *Mol Neurodegener* 2018;13:52. https://doi.org/10.1186/s13024-018-0282-4
52. Nikom D, Zheng S. Alternative splicing in neurodegenerative disease and the promise of RNA therapies. *Nat Rev Neurosci* 2023;24:457-73. https://doi.org/10.1038/s41583-023-00717-6
53. Raghavan NS, Dumitrescu L, Mormino E, *et al*. Association between common variants in RBFOX1, an RNA-binding protein, and brain amyloidosis in early and preclinical Alzheimer disease. *JAMA Neurol* 2020;77:1288-98. https://doi.org/10.1001/jamaneurol.2020.1760
54. Lai Y, Lin X, Lin C, Lin X, Chen Z, Zhang L. Identification of endoplasmic reticulum stress-associated genes and subtypes for prediction of Alzheimer's disease based on interpretable machine learning. *Front Pharmacol* 2022;13:975774. https://doi.org/10.3389/fphar.2022.975774
55. Johnson RJ, Gomez-Pinilla F, Nagel M, *et al.* Cerebral fructose metabolism as a potential mechanism driving Alzheimer's disease. *Front Aging Neurosci* 2020;12:560865. https://doi.org/10.3389/fnagi.2020.560865
56. Sims B, Powers RE, Sabina RL, Theibert AB. Elevated adenosine monophosphate deaminase activity in Alzheimer's disease brain. *Neurobiol Aging* 1998;19:385-91. https://doi.org/10.1016/s0197-4580(98)00083-9
57. Zhuang J, Cai P, Chen Z, *et al.* Long noncoding RNA MALAT1 and its target microRNA-125b are potential biomarkers for Alzheimer's disease management via interactions with FOXQ1, PTGS2 and CDK5. *Am J Transl Res* 2020;12:5940-54. https://doi.org/10.2174/15672050166661907251301 34
58. Li L, Xu Y, Zhao M, Gao Z. Neuro-protective roles of long non-coding RNA MALAT1 in Alzheimer's disease with the involvement of the microRNA-30b/CNR1 network and the following PI3K/AKT activation. *Exp Mol Pathol* 2020;117:104545. https://doi.org/10.1016/j.yexmp.2020.104545
59. More DA, Kumar A. SRSF3: Newly discovered functions and roles in human health and diseases. *Eur J Cell Biol* 2020;99:151099. https://doi.org/10.1016/j.ejcb.2020.151099
60. Jia R, Zheng ZM. Oncogenic SRSF3 in health and diseases. *Int J Biol Sci* 2023;19:3057-76. https://doi.org/10.7150/ijbs.83368
61. Cruz-Rivera YE, Perez-Morales J, Santiago YM, *et al.* A selection of important genes and their correlated behavior in Alzheimer's disease. *J Alzheimers Dis* 2018;65:193-205. https://doi.org/10.3233/jad-170799

Supplementary Table 1. RNA-seq data quality control summary

Sample ID	Total reads	Total mapped reads	Total Uniquely mapped reads	Total Multiple mapped reads
ADA_1	70302118	68407671 (97.31%)	65398538 (95.60%)	3009133 (4.40%)
ADA_2	94377256	91757015 (97.22%)	87977272 (95.88%)	3779743 (4.12%)
ADA_3	90646082	88311652 (97.42%)	84338713 (95.50%)	3972939 (4.50%)
ADB_1	79882954	77467488 (96.98%)	74275294 (95.88%)	3192194 (4.12%)
ADB_2	89077948	86337049 (96.92%)	82653711 (95.73%)	3683338 (4.27%)
ADB_3	82776614	80204597 (96.89%)	76579317 (95.48%)	3625280 (4.52%)
ADB_4	90594184	87967523 (97.10%)	84008796 (95.50%)	3958727 (4.50%)
ADB_5	93636794	90482116 (96.63%)	86508380 (95.61%)	3973736 (4.39%)
C_1	81313822	78481489 (96.52%)	70034875 (89.24%)	8446614 (10.76%)
C_2	87517828	85070554 (97.20%)	73347848 (86.22%)	11722706 (13.78%)
C_3	84534820	81453517 (96.35%)	73982804 (90.83%)	7470713 (9.17%)
C_4	63121448	61250476 (97.04%)	58390265 (95.33%)	2860211 (4.67%)
C_5	87385760	84517632 (96.72%)	81290126 (96.18%)	3227506 (3.82%)

Table Legend
(1) Sample: Sample ID.
(2) Total reads: The number of paired reads after cleaning.
(3) Total mapped reads: Number and percentage of reads mapped to the genome.
(4) Total Uniquely mapped reads: Number of uniquely mapped reads and their percentage among total mapped reads, uniquely mapped reads predominantly originate from mature mRNA.
(5) Total Multiple mapped reads: The number of reads mapped to multiple locations in the reference genome and their percentage among total mapped reads. Multi-mapped reads are primarily composed of rRNA and tRNA.